Emodin promotes the arrest of human lymphoma Raji cell proliferation through the UHRF1-DNMT3A-ΔNp73 pathways

YUN LIN[1], WEIMING CHEN[1], ZHIHONG WANG[1] and PENGWEI CAI[2]

Departments of [1]Hematology and [2]Clinical Laboratory, Fujian Provincial Hospital, Provincial Clinical Medical College of Fujian Medical University, Fuzhou, Fujian 350108, P.R. China

Received June 28, 2016; Accepted May 5, 2017

DOI: 10.3892/mmr.2017.7423

Abstract. Emodin is an active constituent found in the roots and rhizomes of numerous Chinese medicinal herbs. It exerts antitumor activity against Dalton's lymphoma *in vivo*, although the detailed mechanisms by which emodin induces apoptosis remains to be elucidated. The present study aimed to analyze the mechanisms underlying the response to emodin treatment. Using lymphoma Raji cells, an emodin-induced cell proliferating inhibition model was first established, then flow cytometry, western blotting, reverse transcription-quantitative polymerase chain reaction and luciferase reporter assay were performed. It was found that emodin decreased the percentage of Raji cell viability, induced apoptosis, and increased the activation of caspase 3, caspase 9 and poly (ADP-ribose) polymerase through the downregulation of ubiquitin-like protein containing PHD and RING domains 1 (UHRF1). The emodin-induced downregulation of UHRF1 led to an increase in the level of DNA methyltransferase 3A, which in turn inhibited the activity of p73 promoter 2 and decreased the levels of NH2-terminally truncated dominant-negative p73. The treatment of Raji cells with emodin combined with doxorubicin led increased cell death of Raji cells, indicating that emodin may sensitize Raji cells to doxorubicin-induced apoptosis.

Correspondence to: Professor Pengwei Cai, Department of Clinical Laboratory, Fujian Provincial Hospital, Provincial Clinical Medical College of Fujian Medical University, 29 Xinquan Road, Fuzhou, Fujian 350108, P.R. China
E-mail: ppwwcfujian@126.com

Abbreviations: TAp73, transcriptionally active full-length p73; ΔNp73, NH2-terminally truncated dominant-negative p73; UHRF1, ubiquitin-like protein containing PHD and RING domains 1; DNMT3A, DNA methyltransferase 3A

Key words: emodin, NH2-terminally truncated dominant-negative p73, ubiquitin-like protein containing PHD and RING domains 1, p52, apoptosis

Introduction

Emodin ($C_{15}H_{10}O_5$; Fig. 1A), as an active constituent isolated from Chinese traditional herbs, has long been used as a constituent of several prescriptions in traditional Chinese medicine to treat and cure various diseases (1). Emodin has been shown to possess several pharmacological effects, including antibacterial, antiviral and anti-inflammatory effects (2). Emodin has also been shown to inhibit cell growth in different types of tumor cell, including human hepatocellular carcinoma cells, human promyeloleukemic HL-60 cells, human cervical cancer cells and Dalton's lymphoma in mice (3). The potency of emodin in inhibiting cancer cell growth has been reported to be attributed primarily to the induction of cell apoptosis (1). However, the detailed mechanism by which Emodin exerts its anticancer effects remains to be fully elucidated.

As a stress inducible effector, the tumor suppressor gene p53 exerts important effects on the regulation of cellular processes, including cell cycle arrest, apoptosis, autophagy, necroptosis, cell metabolism and senescence (4,5). Under cellular stresses, p53 is stabilized and binds to the promoters of target genes, which results in the transcriptional activation of downstream effectors (6,7). However, p53 is the most frequently mutated tumor suppressor gene in human cancer, and clinical studies have demonstrated that ~50% of tumor cells lack functional p53 (8). P73, a p53 family member, shares significant homology with p53; it is localized to chromosome 1p36.2-3, a region frequently deleted in several tumor types in humans (9,10). The p73 gene encodes two isoforms: Transcriptionally active full-length p73 (TAp73) and NH2-terminally truncated dominant-negative p73 (ΔNp73), which are expressed from two different promoters, p73-promoter-1 and p73-promoter-2 (11,12). TAp73 shares significant similarity with p53, including binding with p53 DNA target sites, transactivation of p53-target genes, and induction of cell cycle arrest and apoptosis; however, the ΔNp73 isoform has opposite effects, as it can inhibit the functions of TAp73 and p53 by competing for binding to the p53/TAp73 DNA target sequence or by forming oligomers with p53/TAp73 (13). Compared with p53, p73 gene mutations are rarely found in human tumors, suggesting the existence of other molecular mechanisms, which may be responsible for the regulation of p73 during oncogenesis.

The proto-oncoproteins MDM2 and MDMX are negative regulators of p53 family members (14). These two proteins contain p53 binding domains, which can bind with p53, export it from the nucleus to the cytosol, and target it for degradation on the 26S proteasome or repress p53 transcriptional targets (15). Although MDM2 and MDMX can also bind with p73 and inhibit P73-transcriptional activity, they do not ubiquitinate p73 (16,17). Therefore, the overexpression of MDM2 or MDMX can lead to suppression of p53/p73 tumor suppressor activities. Additionally, the inhibition of MDM2/MDMX through small interfering (si)RNA or specific inhibitors sensitizes cancer cells to radiotherapy and chemotherapy (18,19), suggesting the MDM2 and MDMX may be therapeutic targets for use in cancer therapies.

In addition to MDM2 family members, other ubiquitin E3 ligases, including ubiquitin-like protein containing PHD and RING domains 1 (UHRF1), can also target p53 and p73 ubiquitination, and suppress p53-dependent transactivation and cell apoptosis in response to DNA damage signals (20,21). Conversely, p53 and p73 can regulate the expression of UHRF1 (22,23). UHRF1 contains several domains, including the N-terminal ubiquitin-like domain (NIRF), plant homeodomain, Set and Ring Associated domain (also known as the YGD domain), and C-terminal RING finger. It can form complexes with histones and non-histone proteins, including promyelocytic leukemia and DNA methyltransferase (DNMT) 1, and exert its E3 ligase activities (24,25). In addition to UHRF1, the UHRF family contains three other members, NIRF, ICBP55 (also known as UHRF3) and ICBP87 (also known as UHRF3), all of which have similar domains to those of UHRF1 (26), suggesting they can also perform UHRF1-like biological functions. However, the activities of NRIF, ICBP55 and ICBP87 remain to be elucidated.

Earlier studies have reported that emodin has antitumor activity against Dalton's lymphoma *in vivo* (27), however, the detailed mechanisms by which emodin induces apoptosis remain to be elucidated. The present study aimed to analyze the mechanisms underlying the response to emodin treatment. Using lymphoma Raji cells, an emodin-induced cell proliferating inhibition model was established and the possible underlying mechanisms were investigated. It was found that emodin downregulated the expression of UHRF1, which in turn suppressed p73 promoter 2 activity through the upregulation of DNMT3A, and increased TAp73/ΔNp73 and cell apoptosis.

Materials and methods

Chemicals. Emodin, 3-(4,5-dimethylthiazol-2-yl)-2,5-diphenyl-2H-tetrazolium bromide (MTT) and dimethyl sulfoxide (DMSO) were purchased from Sigma-Aldrich; Merck KGaA (Darmstadt, Germany). RPMI-1640, Lipofectamine™ 2000, Opti-MEM I medium, TRIzol RNA purification kit and SYBR green I mix, for quantitative polymerase chain reaction (qPCR) analysis, were obtained from Invitrogen; Thermo Fisher Scientific, Inc. (Waltham, MA, USA). Fetal bovine serum (FBS) was from Hyclone; GE Healthcare Life Sciences (Logan, UT, USA). Protein isolation and BCA protein quantification kits were supplied by Beyotime Institute of Biotechnology (Nanjing, China). The Annexin V-fluorescein isothiocyanate (FITC)/propidium iodide (PI) apoptosis detection kit was obtained from MultiSciences Biotechnology (Hangzhou, China). The siRNA sequence targeting UHRF1 (cat. no. sc-270551) was a product of Santa Cruz Biotechnology, Inc. (Dallas, TX, USA). P73-Luc-1, p73-Luc-2 reporter constructs, and the negative control plasmid were obtained from GeneChem Co., Ltd. (Shanghai, China). All specific primers for specific genes and the PrimeScript RT Reagent kit were purchased from Takara Biotechnology Co., Ltd. (Dalian, China).

Antibodies. Primary antibodies against active-caspase 3 (cat. no. 9661L), active-caspase 9 (cat. no. BS7070), active-poly (ADP-ribose) polymerase (PARP; cat. no. AB3620), p53 (cat. no. AP0104), β-actin (cat. no. BS2237) and UHRF1 (cat. no. MB0055) were purchased from Bioworld Technology, Inc. (St. Louis Park, MN, USA). Primary antibodies against ICBP 55 (cat. no. BM1924), ICBP 87 (cat. no. BM2090) and NIRF (cat. no. BM2989) were supplied by Wuhan Boster Biological Technology, Ltd. (Wuhan, China). Primary antibodies against MDM2 (cat. no. sc-812), MDM4 (cat. no. sc-14740), TAp73 (cat. no. sc-9651), ΔNp73 (cat. no. sc-70966), DNMT1 (cat. no. sc-271729), DNMT2 (cat. no. sc-271513), DNMT3A (cat. no. sc-10232), DNMT3B (cat. no. sc-393845) and DNMT3L (cat. no. sc-10239) were all products of Santa Cruz Biotechnology, Inc. IRDye-conjugated anti-rabbit secondary antibody (cat. 611-744-127), IRDye-conjugated anti-mouse secondary antibody (cat. 610-145-121) and IRDye-conjugated anti-goat secondary antibody (cat.605-744-002) were all supplied by Rockland Immunochemicals Inc. (Limerick, PA, USA).

Cell culture and treatment. The Raji cells were obtained from the Cell Bank of the Type Culture Collection of the Chinese Academy of Science (Shanghai, China). The Raji cells were maintained in DMEM supplemented with 10% (v/v) FBS and grown at 37˚C with a humidified 5% CO_2 atmosphere.

Cell proliferation assay. The Raji cells were plated at $1x10^4$ cells per well in a 96-well plate. Following culture for ~24 h, the Raji cells were treated with or without different concentrations of Emodin including 6.25, 12.5, 25 and 50 μM for 4, 8, 12, 24 and 48 h, and cultured at 37˚C with a humidified 5% CO_2 atmosphere. At the end of the experiment, medium was replaced with 100 μl (500 μg/ml) MTT solution and incubated for 4 h at 37˚C. The MTT solution was then removed, and 150 μl DMSO was added to dissolve the formazan crystals. The absorbance at 570 nm for each well was read on a microtiter plate reader (BioTek Instruments, Inc., Winooski, VT, USA). The results were determined as the percentage of the control group.

Flow cytometry. The Raji cells were plated at $2x10^5$ cells per well in a 6-well plate. After 24-48 h, the Raji cells were treated with or without emodin at concentrations of 6.25, 12.5, 25 and 50 μM for 24 h. At the end of the exposure, the Raji cells were collected and washed twice in PBS, an then suspended in 0.5 ml binding buffer containing 5 μl annexin V-FITC and 10 μl PI, and incubated in the dark at room temperature for 30 min. The samples were then analyzed using a FACScan flow cytometer (BD Biosciences, Hercules, CA, USA), and $1x10^4$ events were collected, recorded on a dot plot, and analyzed using ModFit software version 2.0 (Verity Software House, Inc., Topsham, ME, USA).

Western blot analysis. The Raji cells were treated with or without emodin at concentrations of 6.25, 12.5, 25 and 50 μM for 24 h and, at the end of exposure, the Raji cells were harvested for protein extraction. The whole-cell lysate was extracted using a protein isolation kit and protein content was quantified using a BCA protein quantification kit. The lysate proteins (~45 μl; 30 μg) were denatured at 96˚C for 5 min following mixing with 5 μl SDS-loading buffer. The proteins were separated on a 10% SDS-PAGE gel and transferred onto polyvinylidene fluoride membranes (EMD Millipore, Billerica, MA, USA). The membranes were then blocked with TBS containing 5% BSA at 4˚C for 1 h, and then exposed to the specific primary antibodies at 4˚C overnight. This was followed by incubation with the corresponding IRDye-conjugated secondary antibodies (1:5,000 dilution for all) at room temperature for 1 h. The proteins were visualized using the Odyssey Infrared Imaging system with Odyssey v1.2 (LI-COR Biosciences, Lincoln. NE, USA). The relative expression levels of target proteins were normalized to the intensities of β-actin.

Total RNA isolation and reverse transcription-quantitative polymerase chain reaction (RT-qPCR) analysis. The Raji cells were treated with or without emodin at concentrations of 6.25, 12.5, 25 and 50 μM for 24 h. At the end of the experiment, the Raji cells were harvested for RNA extraction using the TRIzol RNA purification kit. First-strand cDNA synthesis was performed using the PrimeScript RT Reagent kit according to the manufacturer's protocol. Amplification was performed using a 7500 Real-Time PCR system (Applied Biosystems; Thermo Fisher Scientific, Inc.), using the SYBR Green RT-PCR kit, according to the manufacturer's protocol [95˚C for 10 sec and 56˚C for 30 sec (45 cycles)]. Relative mRNA expressions were calculated using the $2^{-\Delta\Delta Cq}$ method and normalized to the internal reference gene β-actin (28).

Luciferase reporter assay. The p73 promoter 1 and promoter 2 sequences, synthesized by TransheepBio-Tech Co., Ltd. (Shanghai, China), were cloned into the pGL3-Luc vector (cat. no. 1741; Promega Corporation, Madison, WI, USA) using a Universal GenomeWalker kit supplied by Seebio Biotech (Shanghai) Co., Ltd. (cat. no. 638904; Shanghai, China), according to the manufacturer's protocol. The Raji cells were transfected with the pGL3-Luc vector or a negative vector (pRNL-TK plasmid) using Lipofectamine™ 2000 transfection reagent according to the manufacturer's protocol. Following transfection for 24 h, the Raji cells were treated with or without emodin at concentrations of 6.25, 12.5, 25 and 50 μM for 24 h. At the end of the exposure, the Raji cells were harvested for mRNA isolation, following which cDNA amplification was performed at 95˚C for 10 sec and 55˚C for 30 sec (40 cycles), and RT-qPCR analysis were performed using a two-step method.

UHRF1 siRNA transfection. The Raji cells were plated into 6-well plates at a density of $5x10^5$ cells per well. Following incubation for 24 h, the cells were harvested and diluted to a density of $8x10^5$/ml with DMEM. The Lipofectamine™ 2000 transfection reagent and the UHRF1 siRNA sequence were diluted with Opti-MEM I medium, the final concentrations were 5% and 50 nM, respectively. The above reagents were incubated at 37˚C for 10 min. The two reagents were then mixed and incubated at room temperature for an additional 20 min. Finally, the transfection mixture was added to the 6-well plates. The cell suspensions were overlaid onto the transfection mixture. Following incubation for 4 h, the medium was removed and the cells were cultured with fresh DMEM containing 10% FBS.

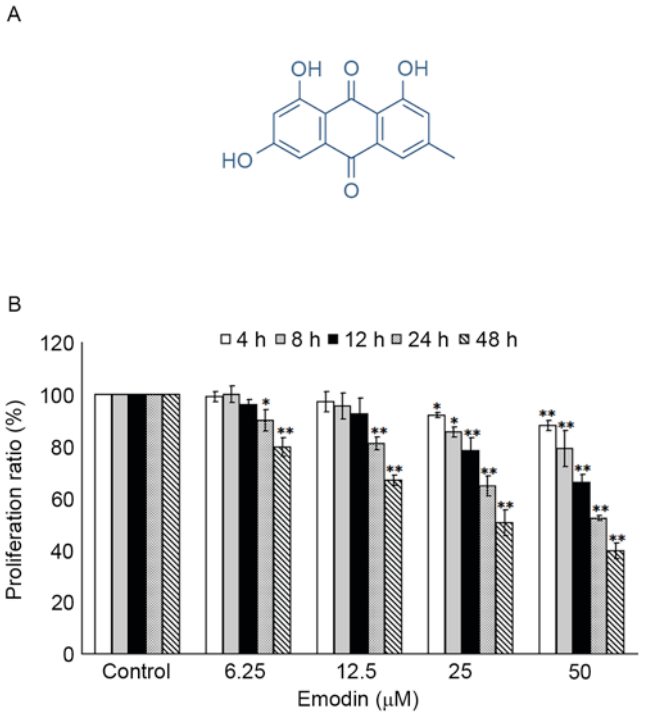

Figure 1. Inhibitory effect of emodin on cell proliferation of Raji cells. (A) Chemical structure of emodin. (B) Dose- and time-responses of emodin on Raji cell proliferation were determined using a 3-(4,5-dimethylthiazol-2-yl)-2, 5-diphenyl-2H-tetrazolium bromide assay following treatment with or without 6.25, 12.5, 25 and 50 μM emodin for 4, 8, 12, 24 and 48 h. *P<0.05 and **P<0.01 vs. the control (0 h) groups.

Results

Emodin decreases the viability of Raji cells. The inhibitory effects of emodin (0, 6.25, 12.5, 25 and 50 μM) on Raji cell viability were evaluated at 4, 8, 12, 24 and 48 h post-treatment. As shown in Fig. 1B, compared with the control groups (untreated groups), significant inhibition of cell viabilities were induced by 6.25-50 μM emodin at 24 and 48 h (P<0.05), whereas 25 and 50 μM emodin significantly decreased Raji cell viabilities at 4, 8 and 12 h. However, no significant cytotoxic effects were found in the 6.25 and 12.5 μM emodin-treated groups of Raji cells over 4-12 h (P>0.05).

Emodin induces the apoptosis of Raji cells. To investigate whether the emodin-induced decrease in cell viability in Raji cells was attribute to apoptosis, the cell death was detected using flow cytometry. As shown in Fig. 2A, compared with the control group, 6.25-50 μM emodin treatment for 24 h significantly increased the apoptosis of Raji cells (P<0.05); these results were further confirmed by the activation of apoptotic effectors caspase 3, PARP and caspase 9, compared with the control group, as shown in Fig. 2B. Treatment with 6.25-50 μM

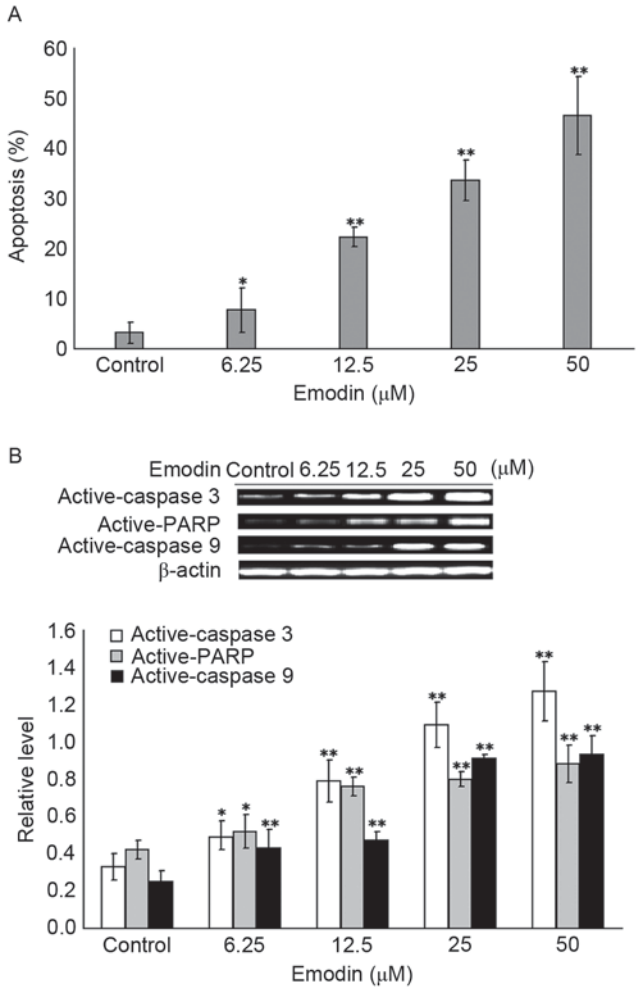

Figure 2. Emodin induces apoptosis of Raji cells. (A) Apoptosis in Raji cells was evaluated using flow cytometry following treatment with or without 6.25, 12.5, 25 and 50 μM emodin for 24 h. (B) Protein levels of active-caspase 3, active-caspase 9 and active-PARP in Raji cells were examined using western blot analysis following treatment with or without 6.25, 12.5, 25 and 50 μM Emodin for 24 h. *P<0.05 and **P<0.01 vs. the untreated control groups. PARP, poly (ADP-ribose) polymerase.

emodin for 24 h significantly increased the protein levels of active-caspase 3, active-PARP and active-caspase 9 (P<0.05).

Emodin induces an increase of TAp73/ΔNp73 in Raji cells through the downregulation of ΔNp73. To investigate whether the emodin-induced apoptosis was associated with p53 or p73, the mRNA and protein expression levels of p53 and p73 in Raji cells were examined using RT-qPCR and western blot analyses. As shown in Fig. 3A, compared with the control group, 6.25-50 μM emodin treatment for 24 h significantly decreased the mRNA levels of p73 (P<0.05), however, no change in the mRNA level of p53 was observed in the emodin-treated groups (P>0.05). Analysis of protein levels, as shown in Fig. 3B, showed that, compared with the control group, the protein levels of ΔNp73, but not of p53 or TAp73, were significantly reduced in the 6.25-50 μM emodin-treated groups (P<0.05). The relative ratio of TAp73 and ΔNp73 (TAp73/ΔNp73) was calculated and is summarized in Fig. 3C. Treatment with 6.25-50 μM emodin for 24 h increased the TAp73/ΔNp73 ratio, compared with that in the control group, and these changes were significant (P<0.05).

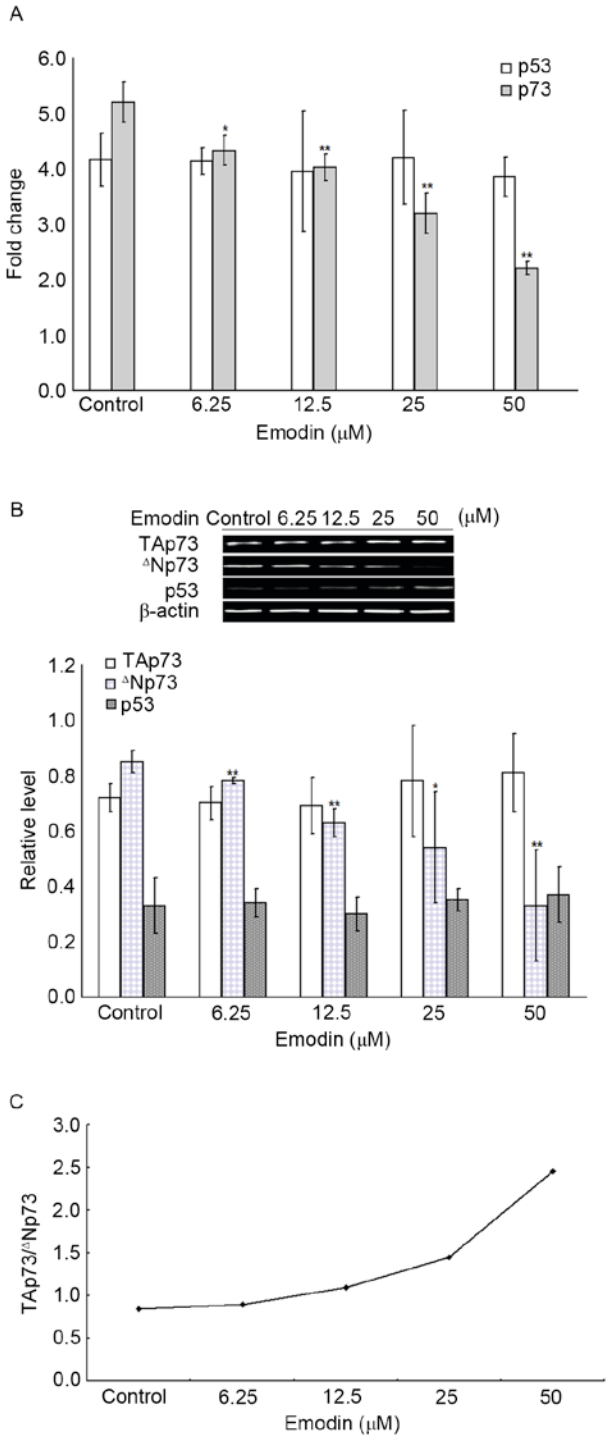

Figure 3. Emodin induces an increase of TAp73/ΔNp73 through downregulation of mRNA and protein levels of ΔNp73. (A) mRNA levels of p53 and p73 in Raji cells were evaluated using reverse transcription-quantitative polymerase chain reaction analysis following treatment with or without 6.25, 12.5, 25 and 50 μM emodin for 24 h. (B) Protein levels of p53, TAp73 and ΔNp73 in Raji cells were evaluated using western blot analysis following treatment with or without 6.25, 12.5, 25 and 50 μM emodin for 24 h. (C) Ratios of TAp73/ΔNp73 in emodin-treated Raji cells were determined. *P<0.05 and **P<0.01 vs. the un-treated control groups. TAp73, transcriptionally active full-length p73; ΔNp73, NH2-terminally truncated dominant-negative p73.

Emodin induces decreased protein levels of UHRF1 in Raji cells. To investigate whether the emodin-induced changes in the expression of ΔNp73 were associated with negative regulators of p53 family members, the mRNA and protein expression levels

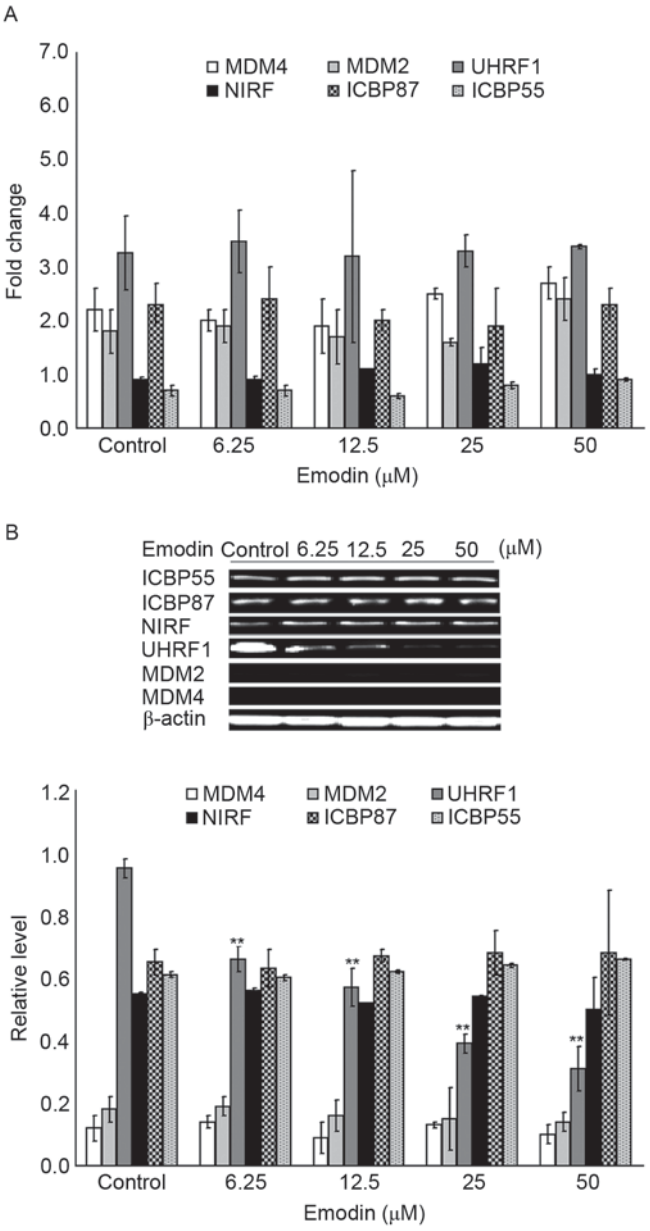

Figure 4. Emodin induces the downregulation of protein levels of UHRF1. (A) mRNA levels of ICBP55, ICBP87, NIRF, UHRF1, MDM2 and MDM4 in Raji cells were evaluated using reverse transcription-quantitative polymerase chain reaction analysis following treatment with or without 6.25, 12.5, 25 and 50 μM emodin for 24 h. (B) Protein levels of ICBP55, ICBP87, NIRF, UHRF1, MDM2 and MDM4 in Raji cells were evaluated using western blot analysis following treatment with or without 6.25, 12.5, 25 and 50 μM emodin for 24 h. **P<0.01 vs. the untreated control groups. UHRF1, ubiquitin-like protein containing PHD and RING domains 1.

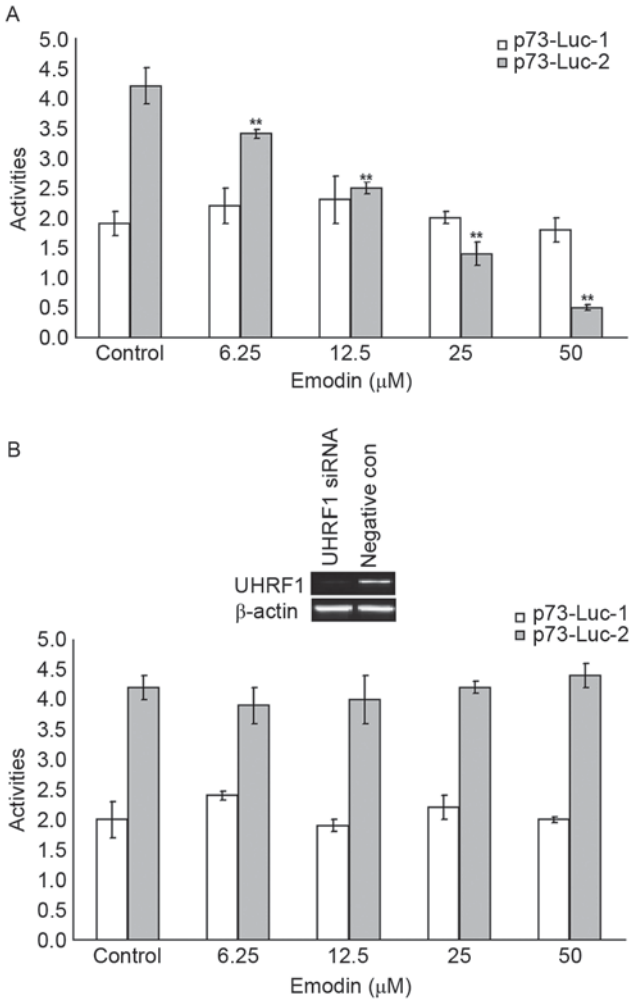

Figure 5. Emodin increases the transcriptional activity of p73-Luc-2 through the inhibition of UHRF1. Raji cells were co-transfected with p73-Luc-1 and p73-Luc-2 plasmids or transfected with negative plasmid, following which stable transfected cells were selected. (A) Stable transfected cells were treated with or without 6.25, 12.5, 25 and 50 μM emodin for 24 h, and transcriptional activities of p73-Luc-1 and p73-Luc-2 were assessed using RT-qPCR analysis. (B) Stable transfected cells were transfected with UHRF1 siRNA or negative siRNA sequence, and the transcriptional activities of p73-Luc-1 and p73-Luc-2 were assessed using RT-qPCR analysis following treatment with or without 6.25, 12.5, 25 and 50 μM emodin for 24 h. **P<0.01 vs. the untreated control groups. UHRF1, ubiquitin-like protein containing PHD and RING domains 1; RT-qPCR, reverse transcription-quantitative polymerase chain reaction; siRNA, small interfering RNA; con, control.

of MDM2, MDM4, ICBP55, ICBP87, NIRF and UHRF1 were examined using RT-qPCR and western blot analyses. As shown in Fig. 4A, compared with the control group, no significant changes were found in the mRNA levels of the target genes in the 6.25-50 μM emodin-treated groups (P>0.05). By contrast, as shown in Fig. 4B, the protein levels of UHRF1 in the 6.25-50 μM emodin-treated groups were decreased, compared with those in the control group, and these changes were significant (P<0.05).

Emodin decreases p73 promoter 2 activity through the inhibition of UHRF1. To investigate the associations of UHRF1 and ΔNp73 in this emodin-treated cell model, the activities of p73 promoter 1 (p73-Luc-1) and p73 promoter 2 (p73-Luc-2) in the Raji cells, and the UHRF1 siRNA-transfected Raji cells were examined using RT-qPCR analysis. As shown in Fig. 5A, compared with the control group, the activities of p73-Luc-2 in the 6.25-50 μM emodin-treated groups were significantly decreased (P<0.05). These emodin-decreased p73-Luc-2 activities were attenuated by UHRF1 siRNA transfection, as shown in Fig. 5B.

UHRF1 inhibits p73-Luc-2 activity through the upregulation of DNMT3A. It is well known that p73 promoter activities can be directly regulated by methylases, therefore, the present study examined the mRNA and protein levels of DNMT1, DNMT2, DNMT3A, DNMT3B and DNMT3L

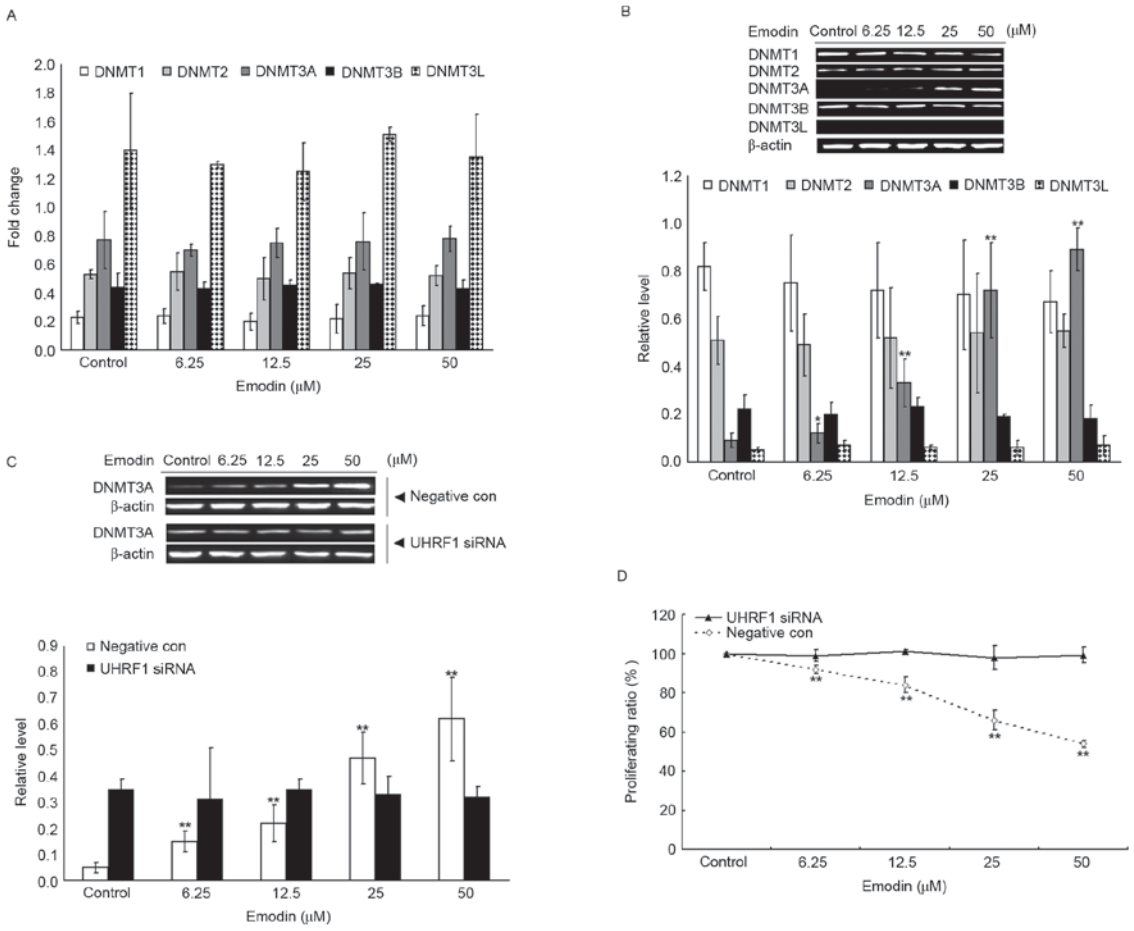

Figure 6. Emodin-induced inhibition of Raji cell proliferation is dependent on the UHRF1-DNMT3A pathway. (A) mRNA levels of DNMT1, DNMT2, DNMT3A, DNMT3B and DNMT3L in Raji cells were evaluated using reverse transcription-quantitative polymerase chain reaction following treatment with or without 6.25, 12.5, 25 and 50 μM Emodin for 24 h. (B) Protein levels of DNMT1, DNMT2, DNMT3A, DNMT3B and DNMT3L in Raji cells was evaluated using western blot analysis following treatment with or without 6.25, 12.5, 25 and 50 μM Emodin for 24 h; (C) Raji cells were transfected with UHRF1 siRNA or negative siRNA sequence, and then treated with or without 6.25, 12.5, 25 and 50 μM Emodin for 24 h. Protein levels of DNMT3A were detected using western blot analysis; (D) Raji cells were transfected with UHRF1 siRNA or negative siRNA sequence, and then treated with or without 6.25, 12.5, 25 and 50 μM Emodin for 24 h. Cell proliferation ratio was evaluated using a 3-(4,5-dimethylthiazol-2-yl)-2,5-diphenyl-2H-tetrazolium bromide assay. *P<0.05 and **P<0.01 vs. the untreated control groups. UHRF1, ubiquitin-like protein containing PHD and RING domains 1; DNMT, DNA methyltransferase; siRNA, small interfering RNA; con, control.

using RT-qPCR and western blot analyses. As shown in Fig. 6A, no significant change in the mRNA levels of the target genes were found in the 6.25-50 μM emodin-treated groups, compared with the control group (P>0.05); however, as shown in Fig. 6B, treatment with 6.25-50 μM emodin significantly increased the protein levels of DNMT3A compared with that in the control group (P<0.05). The associations between UHRF1 and DNMT3A were further investigated, as shown in Fig. 6C and D, and it was found that the emodin-induced upregulation of DNMT3A and decrease of Raji cell viability were attenuated by the knockdown of UHRF1.

Emodin sensitizes doxorubicin-induced Raji cell apoptosis. To further investigate whether emodin exerted a possible synergistic effect in doxorubicin-induced Raji cell apoptosis. The inhibitory effects of emodin (6.25, 12.5 and 25 μM) and doxorubicin (1 μg/ml), alone or in combination were examined. As shown in Fig. 7, compared with the control group (untreated group), both emodin and doxorubicin significantly decreased Raji cell viabilities (P<0.01); when the concentrations of emodin and doxorubicin were added in combination, the decrease in cell viability was more marked (P<0.01).

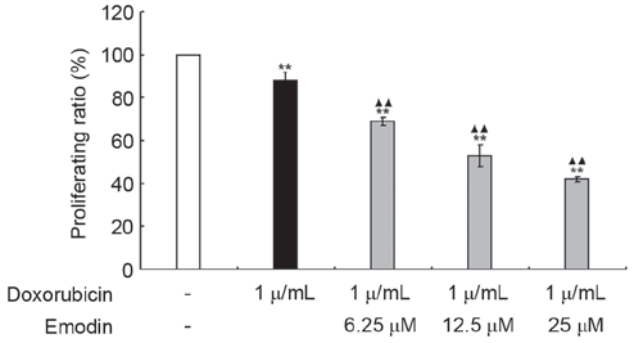

Figure 7. Emodin sensitizes Raji cells to doxorubicin-induced apoptosis. Raji cells were treated with or without emodin and doxorubicin, alone or combination, at indicated concentrations for 24 h. Cell viabilities were evaluated using a 3-(4,5-dimethylthiazol-2-yl)-2,5-diphenyl-2H-tetrazolium bromide assay. **P<0.01, compared with the untreated control group. $^{▲▲}$P<0.01 vs. the 1 μg/ml doxorubicin-treated group.

Discussion

Lymphoma is a blood cell tumor, which develops from lymphatic cells. It is characterized by enlarged lymph nodes, fever, drenching sweats, unintended weight loss, itching and tiredness (29,30). Although lymphoma can be cured as it is usually localized, it can be life threatening, with the majority of victims being children or young adults. Current treatments for lymphoma consist primarily of chemotherapy and radiation therapy; however, their lack of specificity and the existence of toxicity to normal cells are limitations of these methods. Therefore, the identification of more effective anticancer agents to improve tumor specificity and decrease toxicity to normal cells is urgently required. Emodin is a natural compound derived from Chinese traditional herbs, which has been found to induce apoptosis in several human tumor cell lines *in vitro* (3). In agreement with these findings, the present study found that emodin at concentrations of 6.25, 12.5, 25 and 50 μM markedly decreased the viability of Raji cells at 24 h post-treatment. This was further confirmed using flow cytometry and western blot analysis, which demonstrated that emodin concentrations of 6.25, 12.5, 25 and 50 μM induced apoptosis of the Raji cells, and increased the activation of caspase 3, caspase 9 and PARP following 24 h exposure.

p73 is a p53 family member and, unlike the p53 gene which is expressed from a single transcript encoding a single protein, p73 transcribes multiple isoforms (TAp73 and ΔNp73) due to the utilization of two promoters. The overexpression of TAp73 can induce the transactivation of p53-target genes, and inhibit cell proliferation in a p53-like manner through cell apoptosis (9). The overexpression of ΔNp73 has been found in various human cancer cell lines and tumor tissues (10,11). It has been suggested that the ratio between the levels of TAp73 and ΔNp73 (TAp73/ΔNp73) is important in regulating cell fate in response to anticancer agents during chemotherapy (31,32). In the present study, the results confirmed the effects of TAp73/ΔNp73 on cell growth, which was demonstrated by the concurrence of cell apoptosis and increase in TAp73/ΔNp73, the latter attributed to the downregulation of mRNA levels of ΔNp73.

Abnormal DNA hypermethylation catalyzed by DNMTs is critical in regulating gene transcription, gene imprinting and X chromosome inactivation (33,34). The transcription of p73 can be mediated by its two promoters, which locate at CpG islands (35,36). The methylation of cytosine residues of the CpG region results in silencing of the expression of p73 (36,37). A previous study reported that p73 was aberrantly methylated in ~30% of cases of primary acute lymphoblastic leukemia and Burkitt's lymphomas, however, no p73 methylation was detected in normal tissues (38,39). In the present study, a significant association was found between the decreased mRNA expression of ΔNp73 and the downregulation in the activity of p73 promoter 2, suggesting the modification of p73 promoter 2.

The DNMT superfamily contains five members, including DNMT1, DNMT2, DNMT3A, DNMT3B and DNMT3L (40). DNMT1 is primarily responsible for maintaining the methylation status of the genome; DNMT2 encodes a protein responsible for the methylation of tRNA; and DNMT3A, DNMT3B and DNMT3L catalyze the addition of methyl groups to cytosine residues of CpG nucleotides (40). It was previously reported that DNMT1 can regulate p73 promoter methylation in the overexpression of rTCS in Caski cells (41). In the cell model used in the present study, the emodin-induced decrease in the activity of p73 promoter 2 concurred with an increase in the levels of DNMT3A, suggesting an association between p73 promoter methylation and DNMT3A. However, the detailed mechanism for the DNMT3A methylation of p73 requires further investigation.

UHRF1, as an oncogenic factor, is expressed at high levels in various types of cancer (26). It can transmit DNA methylation information from parental cells to daughter cells by discriminating hemimethylated DNA, recruiting DNMT1, and replicating cell nuclear antigen to the correct location to methylate newly synthesized DNA sequences (24,42). UHRF1 can also bind with histone H3, which is tri-methylated at lysine 4 and 9, and maintain the later heterochromatin status (42-44). Therefore, UHRF1 is able to recognize DNA methylation and histone methylation, physically linking these two epigenetic markers. Of note, the present study found that emodin induced the downregulation of UHRF1 and upregulation of DNMT3A, rather than DNMT1. To determine the contribution of the down-regulation of UHRF1 to the upregulation of DNMT3A, the present study inhibited the expression of UHRF1 using siRNA in Raji cells. It was found that the UHFF1 siRNAs effectively knocked down the expression of UHRF1, and significantly attenuated the emodin-induced upregulation of DNMT3A. This suggested the existence of associations between UHFF1 and DNMT3A. However, the detailed mechanism underlying the upregulation of DNMT3A remains to be fully elucidated.

In conclusion, the present study demonstrated that emodin treatment resulted in Raji cell proliferation arrest and apoptosis through an increase in the UHRF1-DNMT3A-TAp73/ΔNp73 pathways. These results suggested that emodin may be used as an anticancer agent to treat the overexpression of UHRF1 in tumors. Further investigations are required to confirm the biological functions of emodin in tumor therapy using animal models.

Acknowledgements

The present study was sponsored by Clinical Medical College of Fujian Medical University.

References

1. Zheng ZH, Hu JD, Chen YY, Lian XL, Zheng HY, Zheng J and Lin MH: Effect of emodin on proliferation inhibition and apoptosis induction in leukemic K562 cells. Zhongguo Shi Yan Xue Ye Xue Za Zhi 17: 1434-1438, 2009 (In Chinese).
2. Lai MY, Hour MJ, Wing-Cheung Leung H, Yang WH and Lee HZ: Chaperones are the target in aloe-emodin-induced human lung nonsmall carcinoma H460 cell apoptosis. Eur J Pharmacol 573: 1-10, 2007.
3. Lai JM, Chang JT, Wen CL and Hsu SL: Emodin induces a reactive oxygen species-dependent and ATM-p53-Bax mediated cytotoxicity in lung cancer cells. Eur J Pharmacol 623: 1-9, 2009.
4. Pastor DM, Irby RB and Poritz LS: Tumor necrosis factor alpha induces p53 up-regulated modulator of apoptosis expression in colorectal cancer cell lines. Dis Colon Rectum 53: 257-263, 2010.
5. Yang SX, Steinberg SM, Nguyen D and Swain SM: p53, HER2 and tumor cell apoptosis correlate with clinical outcome after neoadjuvant bevacizumab plus chemotherapy in breast cancer. Int J Oncol 38: 1445-1452, 2011.
6. Goel A, Fuerst F, Hotchkiss E and Boland CR: Selenomethionine induces p53 mediated cell cycle arrest and apoptosis in human colon cancer cells. Cancer Biol Ther 5: 529-535, 2006.

7. Tu SP, Chi AL, Ai W, Takaishi S, Dubeykovskaya Z, Quante M, Fox JG and Wang TC: p53 inhibition of AP1-dependent TFF2 expression induces apoptosis and inhibits cell migration in gastric cancer cells. Am J Physiol Gastrointest Liver Physiol 297: G385-G396, 2009.
8. Yang L, Zhou Y, Li Y, Zhou J, Wu Y, Cui Y, Yang G and Hong Y: Mutations of p53 and KRAS activate NF-κB to promote chemoresistance and tumorigenesis via dysregulation of cell cycle and suppression of apoptosis in lung cancer cells. Cancer Lett 357: 520-526, 2015.
9. Machado-Silva A, Perrier S and Bourdon JC: p53 family members in cancer diagnosis and treatment. Semin Cancer Biol 20: 57-62, 2010.
10. Basu S and Murphy ME: p53 family members regulate cancer stem cells. Cell Cycle 15: 1403-1404, 2016.
11. Becker K, Pancoska P, Concin N, Vanden Heuvel K, Slade N, Fischer M, Chalas E and Moll UM: Patterns of p73 N-terminal isoform expression and p53 status have prognostic value in gynecological cancers. Int J Oncol 29: 889-902, 2006.
12. Castillo J, Goñi S, Latasa MU, Perugorría MJ, Calvo A, Muntané J, Bioulac-Sage P, Balabaud C, Prieto J, Avila MA and Berasain C: Amphiregulin induces the alternative splicing of p73 into its oncogenic isoform DeltaEx2p73 in human hepatocellular tumors. Gastroenterology 137: 1805-15.e1-4, 2009.
13. Marrazzo E, Marchini S, Tavecchio M, Alberio T, Previdi S, Erba E, Rotter V and Broggini M: The expression of the DeltaNp73beta isoform of p73 leads to tetraploidy. Eur J Cancer 45: 443-453, 2009.
14. Mendoza M, Mandani G and Momand J: The MDM2 gene family. Biomol Concepts 5: 9-19, 2014.
15. Momand J, Villegas A and Belyi VA: The evolution of MDM2 family genes. Gene 486: 23-30, 2011.
16. Madhumalar A, Lee HJ, Brown CJ, Lane D and Verma C: Design of a novel MDM2 binding peptide based on the p53 family. Cell Cycle 8: 2828-2836, 2009.
17. Johnson J, Lagowski J, Lawson S, Liu Y and Kulesz-Martin M: p73 expression modulates p63 and Mdm2 protein presence in complex with p53 family-specific DNA target sequence in squamous cell carcinogenesis. Oncogene 27: 2780-2787, 2008.
18. Guo W, Ahmed KM, Hui Y, Guo G and Li JJ: siRNA-mediated MDM2 inhibition sensitizes human lung cancer A549 cells to radiation. Int J Oncol 30: 1447-1452, 2007.
19. Yu H, Zou Y, Jiang L, Yin Q, He X, Chen L, Zhang Z, Gu W and Li Y: Induction of apoptosis in non-small cell lung cancer by downregulation of MDM2 using pH-responsive PMPC-b-PDPA/siRNA complex nanoparticles. Biomaterials 34: 2738-2747, 2013.
20. Ma J, Peng J, Mo R, Ma S, Wang J, Zang L, Li W and Fan J: Ubiquitin E3 ligase UHRF1 regulates p53 ubiquitination and p53-dependent cell apoptosis in clear cell Renal Cell Carcinoma. Biochem Biophys Res Commun 464: 147-153, 2015.
21. Alhosin M, Abusnina A, Achour M, Sharif T, Muller C, Peluso J, Chataigneau T, Lugnier C, Schini-Kerth VB, Bronner C and Fuhrmann G: Induction of apoptosis by thymoquinone in lymphoblastic leukemia Jurkat cells is mediated by a p73-dependent pathway which targets the epigenetic integrator UHRF1. Biochem Pharmacol 79: 1251-1260, 2010.
22. Colley SM, Iyer KR and Leedman PJ: The RNA coregulator SRA, its binding proteins and nuclear receptor signaling activity. IUBMB Life 60: 159-164, 2008.
23. Dai C, Shi D and Gu W: Negative regulation of the acetyltransferase TIP60-p53 interplay by UHRF1 (ubiquitin-like with PHD and RING finger domains 1). J Biol Chem 288: 19581-19592, 2013.
24. Liang CC and Cohn MA: UHRF1 is a sensor for DNA interstrand crosslinks. Oncotarget 7: 3-4, 2016.
25. Delagoutte B, Lallous N, Birck C, Oudet P and Samama JP: Expression, purification, crystallization and preliminary crystallographic study of the SRA domain of the human UHRF1 protein. Acta Crystallogr Sect F Struct Biol Cryst Commun 64: 922-925 2008.
26. Bronner C, Achour M, Arima Y, Chataigneau T, Saya H and Schini-Kerth VB: The UHRF family: Oncogenes that are drugable targets for cancer therapy in the near future? Pharmacol Ther 115: 419-434, 2007.
27. Singh KB and Trigun SK: Apoptosis of Dalton's lymphoma due to in vivo treatment with emodin is associated with modulations of hydrogen peroxide metabolizing antioxidant enzymes. Cell Biochem Biophys 67: 439-449, 2013.
28. Livak KJ and Schmittgen TD: Analysis of relative gene expression data using real-time quantitative PCR and the 2(-Delta Delta C(T)) method. Methods 25: 402-408, 2001.
29. Poupot M, Pont F and Fournié JJ: Profiling blood lymphocyte interactions with cancer cells uncovers the innate reactivity of human gamma delta T cells to anaplastic large cell lymphoma. J Immunol 174: 1717-1722, 2005.
30. Gujral S, Polampalli SN, Badrinath Y, Kumar A, Subramanian PG, Nair R, Gupta S, Sengar M and Nair C: Immunophenotyping of mature B-cell non Hodgkin lymphoma involving bone marrow and peripheral blood: Critical analysis and insights gained at a tertiary care cancer hospital. Leuk Lymphoma 50: 1290-1300, 2009.
31. Emmrich S, Wang W, John K, Li W and Pützer BM: Antisense gapmers selectively suppress individual oncogenic p73 splice isoforms and inhibit tumor growth in vivo. Mol Cancer 8: 61, 2009.
32. Lau LM, Wolter JK, Lau JT, Cheng LS, Smith KM, Hansford LM, Zhang L, Baruchel S, Robinson F and Irwin MS: Cyclooxygenase inhibitors differentially modulate p73 isoforms in neuroblastoma. Oncogene 28: 2024-2033, 2009.
33. Graça I, Sousa EJ, Baptista T, Almeida M, Ramalho-Carvalho J, Palmeira C, Henrique R and Jerónimo C: Anti-tumoral effect of the non-nucleoside DNMT inhibitor RG108 in human prostate cancer cells. Curr Pharm Des 20: 1803-1811, 2014.
34. Hopfer O, Komor M, Koehler IS, Freitag C, Schulze M, Hoelzer D, Thiel E and Hofmann WK: Aberrant promotor methylation in MDS hematopoietic cells during in vitro lineage specific differentiation is differently associated with DNMT isoforms. Leuk Res 33: 434-442, 2009.
35. Liu K, Zhan M and Zheng P: Loss of p73 expression in six non-small cell lung cancer cell lines is associated with 5'CpG island methylation. Exp Mol Pathol 84 59-63, 2008.
36. Watanabe T, Huang H, Nakamura M, Wischhusen J, Weller M, Kleihues P and Ohgaki H: Methylation of the p73 gene in gliomas. Acta Neuropathol 104: 357-362, 2002.
37. Lai J, Nie W, Zhang W, Wang Y, Xie R, Wang Y, Gu J, Xu J, Song W, Yang F, *et al*: Transcriptional regulation of the p73 gene by Nrf-2 and promoter CpG methylation in human breast cancer. Oncotarget 5: 6909-6922, 2014.
38. Rizzo MG, Giombini E, Diverio D, Vignetti M, Sacchi A, Testa U, Lo-Coco F and Blandino G: Analysis of p73 expression pattern in acute myeloid leukemias: Lack of DeltaN-p73 expression is a frequent feature of acute promyelocytic leukemia. Leukemia 18: 1804-1809, 2004.
39. Kawano S, Miller CW, Gombart AF, Bartram CR, Matsuo Y, Asou H, Sakashita A, Said J, Tatsumi E and Koeffler HP: Loss of p73 gene expression in leukemias/lymphomas due to hypermethylation. Blood 94: 1113-1120, 1999.
40. El-Osta A: DNMT cooperativity-the developing links between methylation, chromatin structure and cancer. Bioessays 25: 1071-1084, 2003.
41. Peng DF, Kanai Y, Sawada M, Ushijima S, Hiraoka N, Kitazawa S and Hirohashi S: DNA methylation of multiple tumor-related genes in association with overexpression of DNA methyltransferase 1 (DNMT1) during multistage carcinogenesis of the pancreas. Carcinogenesis 27: 1160-1168, 2006.
42. Liu X, Gao Q, Li P, Zhao Q, Zhang J, Li J, Koseki H and Wong J: UHRF1 targets DNMT1 for DNA methylation through cooperative binding of hemi-methylated DNA and methylated H3K9. Nat Commun 4: 1563, 2013.
43. Sharif J, Muto M, Takebayashi S, Suetake I, Iwamatsu A, Endo TA, Shinga J, Mizutani-Koseki Y, Toyoda T, Okamura K, *et al*: The SRA protein Np95 mediates epigenetic inheritance by recruiting Dnmt1 to methylated DNA. Nature 450: 908-912, 2007.
44. Hu L, Li Z, Wang P, Lin Y and Xu Y: Crystal structure of PHD domain of UHRF1 and insights into recognition of unmodified histone H3 arginine residue 2. Cell Res 21: 1374-1378, 2011.